journal

J. Am. Ceram. Soc., **91** [10] 3275–3279 (2008)
DOI: 10.1111/j.1551-2916.2008.02670.x

Low-Temperature Sintering and Microwave Dielectric Properties of $Ba_5Nb_4O_{15}$–$BaWO_4$ Composite Ceramics for LTCC Applications

Hao Zhuang, Zhenxing Yue,[†] Fei Zhao, and Longtu Li

State Key Laboratory of New Ceramics and Fine Processing, Department of Materials Science and Engineering,
Tsinghua University, Beijing 100084, China

Low-temperature-sintered composite ceramics in $Ba_5Nb_4O_{15}$–$BaWO_4$ system were prepared by cofiring mixtures of $Ba_5Nb_4O_{15}$ and $BaWO_4$ powders. Thermo-mechanical analysis indicated that a small amount of B_2O_3 addition significantly promoted the densification process and lowered the sintering temperature to ~900°C. X-ray diffraction analysis revealed that $Ba_5Nb_4O_{15}$ and $BaWO_4$ coexisted in the sintered ceramics. With increasing B_2O_3 content, a secondary phase, $BaNb_2O_6$, appeared which affects the microwave dielectric properties. Microwave dielectric properties of the aforementioned compositions were as follows: dielectric constant of 16.8–19.2, $Q \times f$ values of 33 900–50 300 GHz, and a temperature coefficient of the resonant frequency of −3.4 to −8.6 ppm/°C. The chemical compatibility of BNW6502 ceramics with silver during the cofiring process has also been investigated, and no evidence of chemical reaction between Ag and ceramics was observed, indicating that the as-prepared composite ceramics are suitable for low-temperature cofired ceramics applications.

I. Introduction

In the past decades, microwave dielectric ceramics have received much attention because of the rapid growth of wireless communication industry. A large number of ceramic dielectric materials have been developed. A high dielectric constant (ε_r), a high quality factor (Q value), and a low-temperature coefficient of resonant frequency (τ_f) are three key properties required for microwave resonator materials.[1]

Recently, the development of low-temperature cofired ceramics (LTCC) have been stimulated by the benefits offered for the fabrication of miniature multilayer devices involving the cofiring of dielectric and highly conductive metal, such as silver and copper[2,3] and various LTCC materials have been explored.[4] However, most of commercial microwave dielectric materials available exhibiting high quality factor, high dielectric constant, and near-zero temperature coefficient of resonant frequency require high sintering temperature. In order to reduce the sintering temperature of dielectric ceramics, there are several methods commonly explored[4,5]: (1) adding the low melting point compounds such as B_2O_3, V_2O_5; (2) decreasing the particle size of starting materials by chemical methods.[6–8] The first method is widely used to reduce the sintering temperature of commercially developed dielectric ceramics. The low melting point compounds may improve the densification process of ceramics, and then improve the microwave dielectric properties.[9] However, these low melting point compounds may also have a detrimental effect on the microwave dielectric properties due to introducing glassy phase or the formation of secondary phase.

$Ba_5Nb_4O_{15}$, a hexagonal perovskite compound, is one of the most promising materials due to its good dielectric properties of $\varepsilon_r = 39$–40, $Q \times f = 26\,000$ GHz, and $\tau_f = 78$ ppm/°C.[10,11] However, the high sintering temperature (1400°–1450°C) and the large τ_f value limit its application for LTCC microwave devices. Therefore, the further improvement on dielectric properties and sintering behavior is required. Kim *et al.*[12,13] used B_2O_3 to lower the sintering temperature of $Ba_5Nb_4O_{15}$, and decreased the τ_f value through the formation of composite ceramics from $Ba_5Nb_4O_{15}$ and $BaNb_2O_6$.

$BaWO_4$ was reported to have low sintering temperature (~1100°C) and excellent microwave dielectric properties of $\varepsilon_r = 8$, $Q \times f = 57\,500$ GHz, and $\tau_f = -78$ ppm/°C.[14] Because of its large negative τ_f ($= -78$ ppm/°C), we could expect that a dielectric material with near-zero τ_f value and high $Q \times f$ value might be obtained by combining $Ba_5Nb_4O_{15}$ with $BaWO_4$. In our previous studies, the $Ba_5Nb_4O_{15}$–$BaWO_4$ composite ceramics with excellent microwave dielectric properties of $\varepsilon_r = 21.0 \sim 16.9$, $Q \times f = 49\,500 \sim 56\,700$ GHz, and $\tau_f = 8.9 \sim -4.3$ ppm/°C were prepared at low sintering temperature of 1100°C.[15] In order to further reduce the sintering temperature of the composite ceramics, a small of amount of B_2O_3 was added in the present work. In this paper, we investigated the low-temperature sintering behaviors of $Ba_5Nb_4O_{15}$–$BaWO_4$ with B_2O_3 addition and discussed the relationship between the amount of B_2O_3 addition and microwave dielectric properties.

II. Experimental Procedure

The low-temperature-sintered composite ceramics in $Ba_5Nb_4O_{15}$–$BaWO_4$ system were prepared by cofiring mixtures $Ba_5Nb_4O_{15}$ and $BaWO_4$ powders. High-purity (>99.9%) powders of $BaCO_3$, Nb_2O_5, WO_3, and B_2O_3 were used as starting materials. The stoichiometric $Ba_5Nb_4O_{15}$ and $BaWO_4$ powders were synthesized firstly by calcining the oxides mixtures at 1000°C for 4 h and 750°C for 5 h, respectively. Then the composite powders were prepared by mixing the pure $Ba_5Nb_4O_{15}$, $BaWO_4$, and B_2O_3 with weight ratios as listed in Table I. The mixtures were ball milled for 5 h using zirconia balls in an alcohol medium. The slurries were dried, mixed with an appropriate amount of PVA (5 wt%) as a binder, and then screened with a 60 mesh. The screened powders were pressed into cylindrical disks with a diameter of 10 mm and a height of about 5 mm at a pressure of about 2000 kg/cm^2. These pellets were preheated at 600°C for 4 h to expel the binder and then sintered at temperatures from 850° to 1000°C for 4 h in air.

The bulk densities of the samples were measured by the Archimedes method. The relative densities were obtained from the bulk densities and the theoretical densities. The theoretical densities were calculated from the following equation:

$$\rho = \frac{W_1 + W_2}{W_1/\rho_1 + W_2/\rho_2} \tag{1}$$

P. K. Davies—contributing editor

Manuscript No. 24659. Received May 12, 2008; approved July 23, 2008.

This work was supported by the National Science Foundation of China (Grant Nos. 50672043, 50621201, and 50632030), and the Ministry of Science and Technology of China through 973-Project under 2002CB613307.

[†] Author to whom correspondence should be addressed. e-mail: yuezhx@tsinghua.edu.cn

Table I. The $Ba_5Nb_4O_{15}$, $BaWO_4$, and B_2O_3 Content of all Samples

Sample	$Ba_5Nb_4O_{15}$ (wt%)	$BaWO_4$ (wt%)	B_2O_3 (wt%)
BNW6502	35	65	0.2
BNW6002	40	60	0.2
BNW6004	40	60	0.4
BNW6006	40	60	0.6

Where ρ_1 and ρ_2 are the theoretical density of $Ba_5Nb_4O_{15}$ and $BaWO_4$, 6.32 g/cm^3 for $Ba_5Nb_4O_{15}$ phase and 6.38 g/cm^3 for $BaWO_4$ phase.[16] W_1 and W_2 are the weight fraction of $Ba_5Nb_4O_{15}$ and $BaWO_4$.

The crystalline phases of the sintered samples were determined by X-ray diffraction (XRD), using Cu$K\alpha$ radiation (Rigaku D/Max-2500, Tokyo, Japan). Shrinkage curve was determined using thermo-mechanical analysis (TMA) (SETARAM TGA TMA DSC) technique. The microstructures of sintered ceramics were observed by scanning electron microscopy (SEM). The composition analysis was performed using energy-dispersive spectroscopy (EDS: model INCA, Oxford Instruments, Oxford, U.K.). A network analyzer (HP8720ES, Hewlett-Packard, Santa Rosa, CA) was used to measure the microwave dielectric properties. The dielectric constants were measured using the Hakki and Coleman[17] postresonator method by exciting the TE011 resonant mode of the dielectric resonators using the electric probe of an antenna as suggested by Courtney.[18] The measuring error is about 1%. The unloaded quality factors were measured using the TE01d mode in the cavity method.[19] All measurements were made in the frequency range of 8–11 GHz at room temperature. The temperature coefficients of the resonant frequencies (τ_f) were obtained in the temperature range from 20° to 80°C. The τ_f values were calculated by the following relationship:

$$\tau_f = \frac{f_2 - f_1}{f_1(T_2 - T_1)} \qquad (2)$$

where f_1 and f_2 are the resonant frequencies at T_1 and T_2, respectively.

For cofiring experiments, the ceramic slurries combined ceramic powders with organic additions were tape-casted to form a green film. Silver electrode was screen-printed onto the green film using a screen printer. The samples were cofired at 900°C for 4 h in the air. SEM and EDS were used to characterize the diffusion of silver.

III. Results and Discussion

Figure 1 shows the XRD patterns of the B_2O_3-doped $Ba_5Nb_4O_{15}$–$BaWO_4$ ceramics sintered at 900°C for 4 h. It is clearly seen that all of the peaks could be indexed in terms of the $Ba_5Nb_4O_{15}$ (○) and $BaWO_4$ (▼). For the samples BNW6002 and BNW6502 with 0.2 wt% B_2O_3, the crystalline phases were $Ba_5Nb_4O_{15}$ and $BaWO_4$, and there was no evidence of any secondary phase present, which is also observed in the undoped samples in our previous work.[15] This suggests that two phases, $Ba_5Nb_4O_{15}$ and $BaWO_4$, coexisted in the present LTCC materials. The coexistence of $Ba_5Nb_4O_{15}$ and $BaWO_4$ in the sintered bodies might be attributed to the different crystallized structures of two phases and the different coordination numbers (CN) of Nb and W in their crystal structures. $Ba_5Nb_4O_{15}$ has a hexagonal perovskite structure in which the CN of Nb^{5+} is 6, while $BaWO_4$ has a scheelite structure with four coordination of W^{6+}. The differences in the crystal structure and the CN of Nb and W limit the formation of solid solution between $Ba_5Nb_4O_{15}$ and $BaWO_4$, thus $Ba_5Nb_4O_{15}$ and $BaWO_4$ can coexist in the as-sintered ceramics. With increasing B_2O_3 content, for samples BNW6004 with 0.4 wt% B_2O_3 and BNW6006 with 0.6 wt% B_2O_3, peaks for $BaNb_2O_6$ indicated by * appeared. Taking into account the main difference between the above samples was the B_2O_3 content, the formation of the Nb-rich barium metaniobate, $BaNb_2O_6$, may be attributed to the reaction of $Ba_5Nb_4O_{15}$ and B_2O_3. Kim *et al.*[12,13] also found that the addition of B_2O_3 in $Ba_5Nb_4O_{15}$ could result in the formation of $BaNb_2O_6$. Moreover, the $BaNb_2O_6$ has two polymorphic phases: hexagonal and orthorhombic.[20] Recent literature[20] revealed that the hexagonal $BaNb_2O_6$ was a low-temperature phase, and could be transformed to the orthorhombic phase over a broad temperature range >1150°C. So in the present system, when the B_2O_3 amount is over 0.4 wt%, a very small amount of $BaNb_2O_6$ existed as the hexagonal phase, as shown in Fig. 1 (inset).

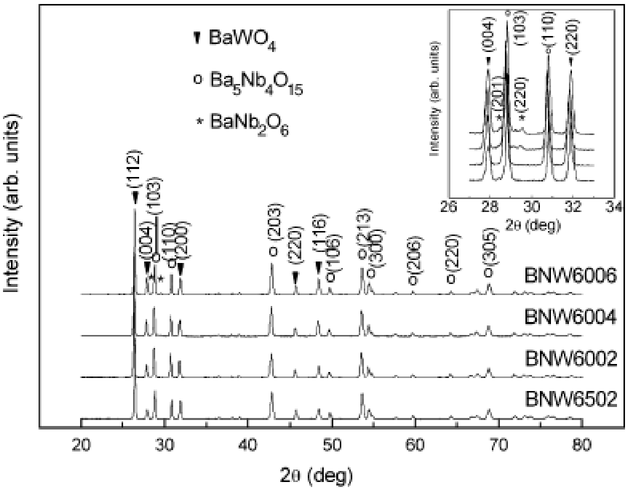

Fig. 1. X-ray diffraction patterns of $Ba_5Nb_4O_{15}$–$BaWO_4$ ceramics sintered at 900°C for 4 h. Inset shows secondary phase reflections at around $2\theta\sim29°$ and 30°.

In order to evaluate the sintering behavior of the composite ceramics, the TMA technique was used to characterize the sintering shrinkage. Figure 2 shows the shrinkage and shrinking rate as a function of temperature for the pressed samples. It

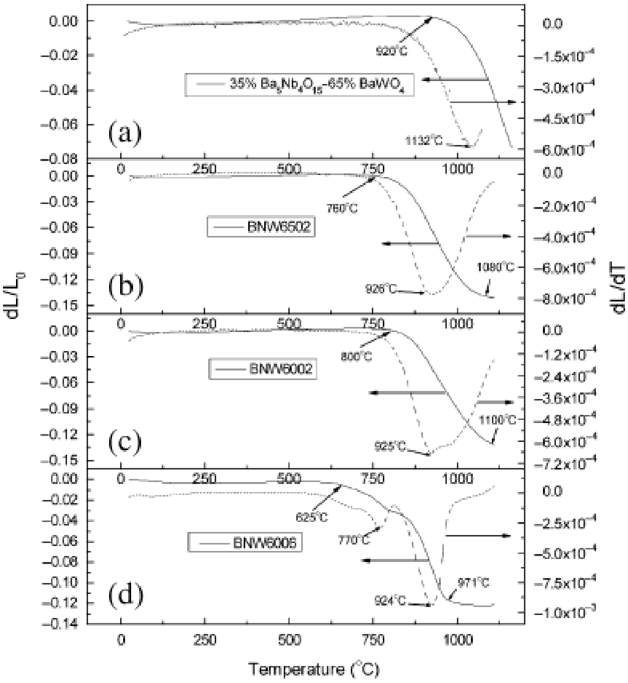

Fig. 2. Dilatometric curves (solid line, dL/l_0) and their derivatives (dotted line, dL/dT) of $Ba_5Nb_4O_{15}$–$BaWO_4$ ceramics (a) 35%$Ba_5Nb_4O_{15}$–65%$BaWO_4$ without B_2O_3 addition, (b) BNW6502, (c) BNW6002, and (d) BNW6006.

demonstrates that the onset of shrinkage takes place at ~920°C and a maximum densification rate occurs at ~1130°C for sample without B_2O_3 (as shown in Fig. 2(a)). With the addition of small amount of B_2O_3, as shown in Figs. 2(b) and (c), the densification rate is a little faster than that of the undoped sample. The highest densification rate occurs at ~925°C, which is much lower than that of the undoped sample. These experiments suggest that a small amount of B_2O_3 addition is effective to lower the sintering temperature and promote the densification process of $Ba_5Nb_4O_{15}$–$BaWO_4$ composite ceramics. Thus, the low-temperature sintering could be achieved at about 900°C for the present composite ceramics, which could meet the requirement for LTCC applications. From Figs. 2(b) and (c), it can also be observed that the densification range of BNW6002 is large than that of BNW6502, which may be due to the different sintering temperature of $Ba_5Nb_4O_{15}$ (1400°C) and $BaWO_4$ (1100°C). Compared with sample BNW6502, BNW6002 contains more $Ba_5Nb_4O_{15}$, which has a negative effect on the sintering temperature and results in the larger densification range of BNW6002. The addition of large amount of B_2O_3 (Fig. 2(d)) produces two minima on the densification rate curve, which indicates two stages of the sintering process. Noticeable densification starts at about 625°C, which is much lower than the undoped sample (~920°C). The first peak, at 770°C, may be related to the liquid-phase sintering with a high densification rate, while the second peak, at 925°C, signifies the final densification process.[9] A reduced densification rate exists in the temperature region of 770°–925°C, which implies that the densification is hindered by the formation of pores which may be due to the pore coalescence upon sintering with an excessive of B_2O_3.[9] This result suggests that no more than 1 wt% of B_2O_3 is necessary for sintering to occur at temperatures <925°C with minimal porosity.

Figure 3 shows the SEM micrographs for sintered surface of the composite ceramics sintered at 900°C. The evolution of the microstructures relative to the B_2O_3 content was observed from Figs. 3(a)–(c). The addition of B_2O_3 significantly improved the grain growth of the $Ba_5Nb_4O_{15}$–$BaWO_4$ mixture. From Fig. 3(a), small pores are observed in the sample BNW6002; these pores may be attributed to the poor sinterability with low B_2O_3 content (0.2 wt%). With increasing B_2O_3 content, dense ceramics can be observed. Furthermore, the grain size increases with increasing B_2O_3 content. This suggests that the sinterability of the $Ba_5Nb_4O_{15}$–$BaWO_4$ ceramics can be improved by B_2O_3 addition. It is noted from Fig. 3(d) that the grain size of BNW6502 is much larger than that of BNW6002 (Fig. 3(a)). The main difference between the two samples is the $Ba_5Nb_4O_{15}$ content. The sample BNW6002 contains more $Ba_5Nb_4O_{15}$, which has much higher sintering temperature (1400°C) compared with $BaWO_4$ (1100°C). The existence of $Ba_5Nb_4O_{15}$ may suppress the grain growth of the $Ba_5Nb_4O_{15}$–$BaWO_4$ ceramics. It can be also observed that there exist two types of grains in all the above samples: one is the large grains (~3 μm) and the other is the small grains (<1 μm). To confirm the composition of the two types of grains of the sample BNW6502, EDS was used. The results are shown in Fig. 4. The results show that the larger grains are composed of pure $BaWO_4$ and the smaller ones are composed of pure $Ba_5Nb_4O_{15}$, which may be due to much lower sintering temperature of $BaWO_4$ (1100°C) compared with that of $Ba_5Nb_4O_{15}$ (1400°C). At low sintering temperature, $BaWO_4$ grains grow superiorly.

The dielectric properties at microwave frequency were measured on the sintered ceramic samples and the results are listed in Table II. In order to indicate clearly the effects of sintering temperature on the microwave dielectric properties, the variations of dielectric constants and $Q \times f$ values of $Ba_5Nb_4O_{15}$–$BaWO_4$ ceramics with sintering temperature are shown in Fig. 5. From Fig. 5(a), it can be observed that the dielectric constant increases with increasing temperature initially, and then saturated (for sample BNW6502 and BNW6006) or slightly dropped (for sample BNW6002 and BNW6004). As the relative densities of the samples are all above 95%, the effect of porosity on the microwave dielectric properties can be neglected. Thus, for samples BNW6002, BNW6004, and BNW6006, the dielectric

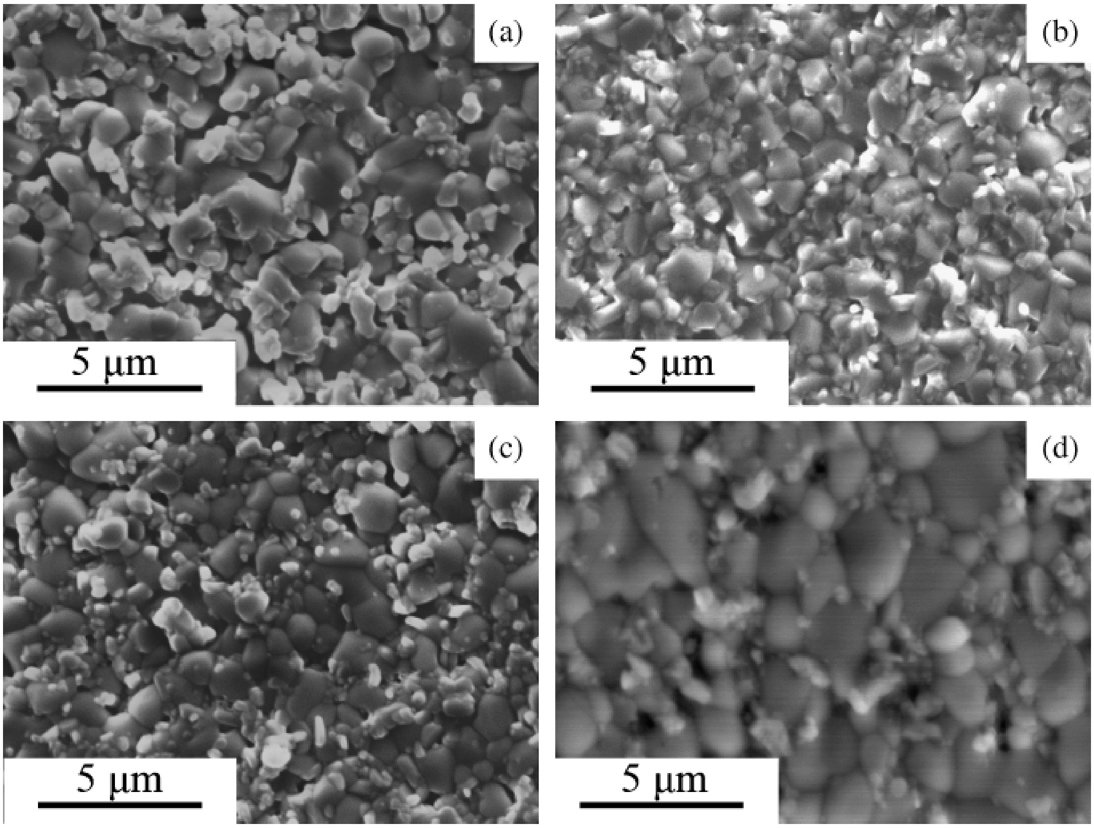

Fig. 3. Scanning electron microscopy photographs of the as-fired surface of $Ba_5Nb_4O_{15}$–$BaWO_4$ ceramics sintered at 900°C. (a) BNW6002, (b) BNW6004, (c) BNW6006, and (d) BNW6502.

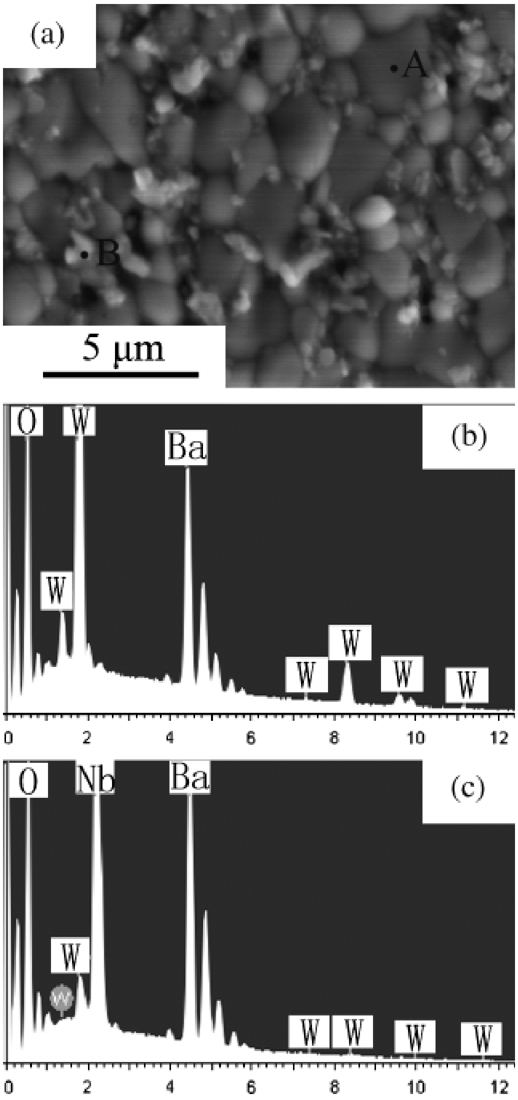

Fig. 4. Scanning electron microscopy photograph of the sample BNW6502 sintered at 900°C and its EDS spectrum. (a) BNW6502 sintered at 900°C, (b) EDS spectrum of A, and (c) EDS spectrum of B.

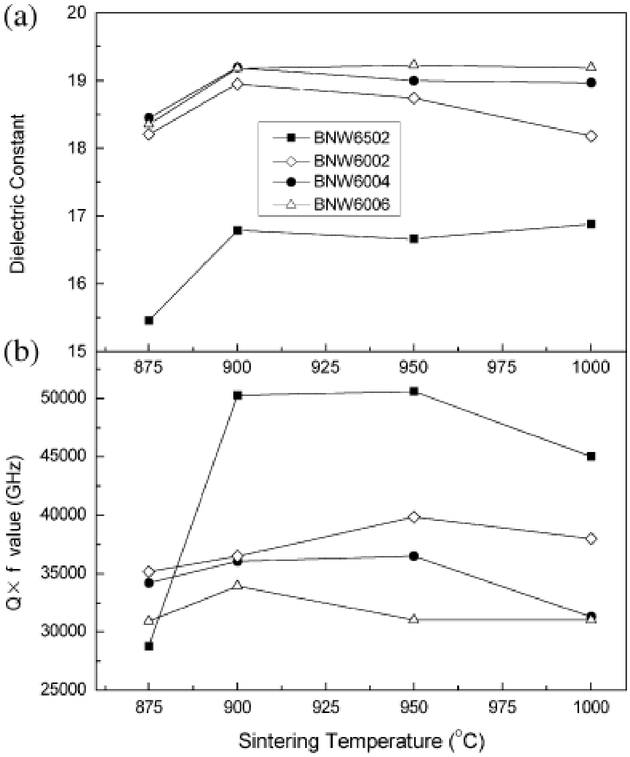

Fig. 5. Microwave dielectric properties of $Ba_5Nb_4O_{15}$–$BaWO_4$ ceramics sintered at different temperatures, (a) dielectric constant and (b) $Q \times f$ value.

constants are mainly affected by the secondary phase—hexagonal $BaNb_2O_6$ and the glassy phase caused by B_2O_3 addition. According to XRD data shown in Fig. 1, diffraction peaks associated with hexagonal $BaNb_2O_6$ appeared during low-temperature firing of $Ba_5Nb_4O_{15}$–$BaWO_4$ when the addition of B_2O_3 is over 0.4 wt%. Hexagonal $BaNb_2O_6$ is reported to have microwave dielectric properties of $Q \times f = 4000$ GHz, $\varepsilon_r = 42$, and $\tau_f = -800$ ppm/°C.[20] The relative high dielectric constant (~ 42) of $BaNb_2O_6$ will cause the increase of dielectric constant of composites with increasing B_2O_3 content. However, the increase of B_2O_3 will increase the glassy phase, which will cause the decrease of dielectric constant. Considering the both effects of $BaNb_2O_6$ (positive) and glassy phase (negative) on the dielectric constant of the samples, the slight increase in dielectric constant with increasing B_2O_3 is observed for BNW6002, BNW6004, and BNW6006. Noticeably, the dielectric constant of BNW6502 is much lower than that of BNW6002, although they have the same amount of B_2O_3. The difference between the dielectric constants may be due to the different amount of $BaWO_4$, which is reported to have microwave dielectric properties of $\varepsilon_r = 8$, $Q \times f = 57\,500$ GHz, and $\tau_f = -78$ ppm/°C.[14] BNW6502 contains more $BaWO_4$ than BNW6002 which induces the lower dielectric constant of BNW6502.

Table II. Relative Density and Microwave Dielectric Properties of $Ba_5Nb_4O_{15}$–$BaWO_4$ Ceramics Sintered at 900°C

Sample	Relative Density (%)	ε_r	$Q \times f$ (GHz)	τ_f (ppm/°C)
BNW6502	96.3	16.8	50 300	−6.4
BNW6002	95.4	18.9	36 500	−3.4
BNW6004	96.7	19.1	36 000	−6.3
BNW6006	96.5	19.2	33 900	−8.6

Figure 5(b) shows the $Q \times f$ values of $Ba_5Nb_4O_{15}$–$BaWO_4$ ceramics with different sintering temperature. It is observed that the maximum $Q \times f$ values can be obtained around 900°–950°C. The $Q \times f$ values increase with increasing temperature initially, then reached the maximum value, finally, dropped or remain nearly unchanged at 1000°C. This phenomenon agrees well with the dilatometric curves (See Fig. 2). The samples are over-heated when sintered at 1000°C. It can also be observed that the optimized sintering temperature of BNW6002 is 950°C, while that of BNW6004 and 6003 is 900°C. This agrees well with the density curves, which is not provided here. For samples BNW6002, BNW6004, and BNW6006 sintered at optimized temperature, the $Q \times f$ values decrease from 39 800 to 33 900 GHz with increasing B_2O_3 content. As the samples' relative densities are all above 95%, the effect of the density on the $Q \times f$ values of $Ba_5Nb_4O_{15}$–$BaWO_4$ ceramics should be neglected. The decrease of $Q \times f$ values may be resulted in the formation of the $BaNb_2O_6$, whose $Q \times f$ value is only ~ 4000 GHz. Moreover, the addition of B_2O_3 may cause the formation of glassy phase which may also contribute to the slight decrease of the $Q \times f$ values. The $Q \times f$ value of BNW6502 (50 300 GHz) is different from the other samples again. This may be due to the more content of the low dielectric loss phase, $BaWO_4$. Further more, the larger grain size of BNW6502 observed in Fig. 3(e) may also contribute to the higher $Q \times f$ value. For samples BNW6002, BNW6004, and BNW6006, it can be seen that the τ_f values decrease from −3.4 to −8.6 ppm/°C. This may be due to large negative τ_f value of $BaNb_2O_6$ (−800 ppm/°C). However, as the $BaNb_2O_6$ amount is small, the decreases of τ_f values are small.

For compatibility tests, the silver electrode was screen-printed onto BNW6502 green bodies using a screen printer. Figure 6

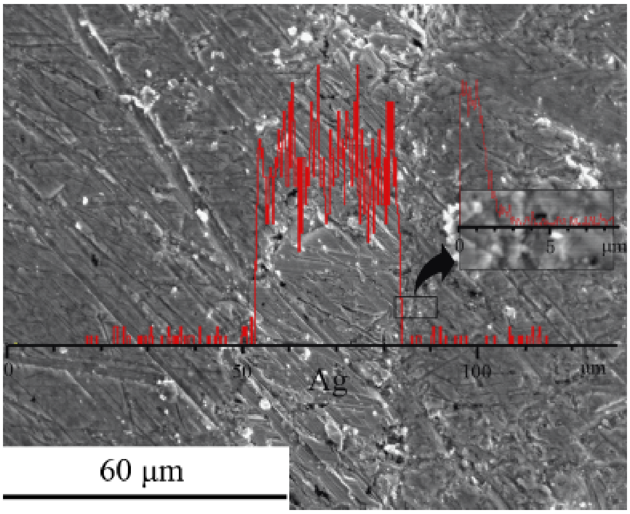

Fig. 6. Scanning electron microscopy photograph and the EDS analysis of BNW6502 cofired with Ag in the air at 900°C for 4 h. Inset shows the EDS analysis at the interface between Ag and BNW6502.

shows the SEM image and the EDS analysis of the sample. It can be seen that the silver electrodes has good chemical compatibility and coheres closely with BNW6502 ceramics. The interface between BNW6502 and silver electrode is clear and further analysis is performed on the Ag and BNW6502 interface. The result is shown in the inset of Fig. 6. It can be seen that the Ag penetration depth is ~1.5 μm. Figure 7 shows the XRD patterns of BNW6502 ceramic and mixture of BNW6502 and Ag ceramic. No secondary phases are observed in Fig. 7, implying that the reaction of low-fired $Ba_5Nb_4O_{15}$–$BaWO_4$ with Ag electrodes did not occur. This result is in accordance with the SEM and EDS results as shown in Fig. 6. Therefore, $Ba_5Nb_4O_{15}$–$BaWO_4$ could be selected as suitable candidates for LTCC materials, because of low sintering temperature, good microwave dielectric properties, and compatibility with electrodes.

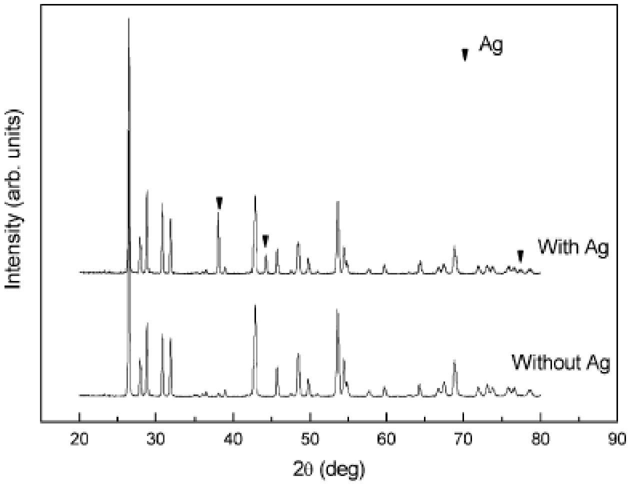

Fig. 7. X-ray diffraction patterns of BNW6502 ceramic and mixture of BNW6502 and Ag sintered at 900°C for 4 h in the air.

IV. Conclusions

B_2O_3 can significantly lower the sintering temperature of $Ba_5Nb_4O_{15}$–$BaWO_4$ ceramics from ~1100° to ~900°C. It is found that large addition of B_2O_3 will cause the formation of hexagonal $BaNb_2O_6$, which affects the microwave dielectric properties of $Ba_5Nb_4O_{15}$–$BaWO_4$ ceramics. The amount of $BaWO_4$ also influences the sintering behavior and microwave dielectric properties of the ceramics. The low-temperature fired $Ba_5Nb_4O_{15}$–$BaWO_4$ possesses excellent microwave dielectric properties: ε_r of 16.8~19.2, $Q \times f$ values of 33 900~50 300 GHz, and a τ_f between −3.4 and ~−8.6 ppm/°C. Also, this material is compatible with Ag electrodes, therefore, is suitable for LTCC applications.

References

[1] W. Wersing, "Microwave Ceramics for Resonators and Filters," *Curr. Opin. Solid State Mater. Sci.*, **1**, 715–31 (1996).

[2] J. Wang, Z. X. Yue, Z. L. Gui, and L. T. Li, "Low Temperature Sintered $ZnNb_2O_6$ Microwave Dielectric Ceramics Doped with ZnO–V_2O_5 Additions," *J. Mater. Sci.*, **40**, 6581–3 (2005).

[3] K. Wakino, T. Nishikawa, Y. Ishikawa, and H. Tamura, "Dielectric Resonator Materials and their Applications for Mobile Communication Systems," *Br. Ceram. Trans. J.*, **89**, 39–43 (1990).

[4] M. T. Sebastian and H. Jantunen, "Low Loss Dielectric Materials for LTCC Applications: A Review," *Int. Mat. Rev.*, **53**, 57–90 (2008).

[5] R. Umemura, H. Ogawa, H Ohsato, A. Kan, and A. Yokoi, "Microwave Dielectric Properties of Low-Temperature Sintered $Mg_3(VO_4)_2$ Ceramic," *J. Eur. Ceram. Soc.*, **25**, 2865–70 (2005).

[6] K. P. Surendran, P. C. R. Varma, and M. R. Varma, "Solid State and Solution Synthesis of $Ba(Mg_{1/3}Ta_{2/3})O_3$: A Comparative Study," *Mater. Res. Bull.*, **42**, 1831–44 (2007).

[7] A. B. Gaikwad, S. C. Navale, V. Samuel, A. V. Murugan, and V. Ravi, "A Co-Precipitation Technique to Prepare $BiNbO_4$, $MgTiO_3$ and $MgTa_2O_9$ Powders," *Mater. Res. Bull.*, **41**, 347–53 (2006).

[8] J. Pei, Z. X. Yue, F. Zhao, Z. L. Gui, and L. T. Li, "Effects of Silver Doping on the Sol-Gel Derived $Ba_4(Nd_{0.7}Sm_{0.3})_{9.33}Ti_{18}O_{54}$ Microwave Dielectric Ceramics," *J. Am. Ceram. Soc.*, **90**, 3131–7 (2007).

[9] H. T. Kim, S. H. Kim, S. Nahm, and J. D. Byun, "Low-Temperature Sintering and Microwave Dielectric Properties of Zinc Metatitanate–Rutile Mixtures Using Boron," *J. Am. Ceram. Soc.*, **82** [11] 3043–8 (1999).

[10] R. Ratheesh, M. T. Sebastian, P. Mohanan, M. E. Tobar, J. Hartnett, R. Woode, and D. G. Blair, "Microwave Characterisation of $BaCe_2Ti_5O_{15}$ and $Ba_5Nb_4O_{15}$ Ceramic Dielectric Resonators Using Whispering Gallery Mode Method," *Mater. Lett.*, **45**, 279–85 (2000).

[11] C. Vineis, P. K. Davies, T. Negas, and S. Bell, "Microwave Dielectric Properties of Hexagonal Perovskites," *Mater. Res. Bull.*, **31**, 431–7 (1996).

[12] D. W. Kim, K. S. Hong, C. S. Yoon, and C. K. Kim, "Low-Temperature Sintering and Microwave Dielectric Properties of $Ba_5M_4O_{15}$–$BaNb_2O_6$ Mixtures for LTCC Applications," *J. Eur. Ceram. Soc.*, **23**, 2597–601 (2003).

[13] D. W. Kim, J. R. Kim, S. H. Yoon, K. S. Hong, and C. K. Kim, "Microwave Dielectric Properties of Low-Fired $Ba_5Nb_4O_{15}$," *J. Am. Ceram. Soc.*, **85**, 2759–62 (2002).

[14] S. H. Yoon, D. W. Kim, S. Y. Cho, and K. S. Hong, "Investigation of the Relations Between Structure and Microwave Dielectric Properties of Divalent Metal Tungstate Compounds," *J. Eur. Ceram. Soc.*, **26**, 2051–4 (2006).

[15] H. Zhuang, Z. X. Yue, F. Zhao, and L. T. Li, "Microstructure and Microwave Dielectric Properties of $Ba_5Nb_4O_{15}$–$BaWO_4$ Composite Ceramics," *J. Alloy. Compd.* doi: 10.1016/j.jallcom.2008.04.073.

[16] Z. Q. Tian, H. X. Liu, H. T. Yu, and S. X. Ouyang, "Effect of $BaWO_4$ on Microstructure Microwave Dielectric Properties of $Ba(Mg_{1/3}Nb_{2/3})O_3$," *Mater. Chem. Phys.*, **86**, 228–32 (2004).

[17] B. W. Hakki and P. D. Coleman, "A Dielectric Resonator Method of Measuring Inductive in the Millimeter Range," *IRE Trans. Microwave Theory Tech.*, **MMT-8**, 402–10 (1960).

[18] W. E. Courtney, "Analysis and Evaluation of a Method of Measuring the Complex Permittivity and Permeability of Microwave Insulators," *IEEE Trans. Microwave Theory Tech.*, **MMT-18**, 476 (1970).

[19] J. Krupka, K. Derzakowski, B. Riddle, and J. B. Jarbis, "A Dielectric Resonator for Measurements of Complex Permittivity of Low Loss Dielectric Materials as a Function of Temperature," *Meas. Sci. Technol.*, **9**, 1751–6 (1998).

[20] D. W. Kim, H. B. Hong, K. S. Hong, C. K. Kim, and D. J. Kim, "The Reversible Phase Transition and Dielectric Properties of $BaNb_2O_6$ Polymorphs," *Jpn. J. Appl. Phys.*, **41**, 6045–8 (2002). □